Identifying and Indexing Icosahedral Quasicrystals from Powder Diffraction Patterns

Peter J. Lu,[1,*] Kenneth Deffeyes,[2] Paul J. Steinhardt,[1] and Nan Yao[3]

[1]*Department of Physics, Princeton University, Princeton, New Jersey 08544*
[2]*Department of Geology, Princeton University, Princeton, New Jersey 08544*
[3]*Princeton Materials Institute, Princeton University, Princeton, New Jersey 08544*

(Received 29 August 2001; published 13 December 2001)

We present a scheme to identify quasicrystals based on powder diffraction data and to provide a standardized indexing. We apply our scheme to a large catalog of powder diffraction patterns, including natural minerals, to look for new quasicrystals. Based on our tests, we have found promising candidates worthy of further exploration.

DOI: 10.1103/PhysRevLett.87.275507 PACS numbers: 61.10.Nz, 61.44.Br

Quasicrystals are solids whose diffraction patterns exhibit a rotational symmetry, such as fivefold symmetry, that is forbidden for periodic crystals [1]. The forbidden symmetry is related to the fact that the atoms are arranged quasiperiodically. Quasiperiodic translational order has physical consequences. For example, since electrons and phonons in quasicrystals do not encounter a periodic potential, quasicrystals have unusual resistive and elastic properties, and these have been exploited in several applications [2]. To date, known quasicrystals have been found by serendipity or by probing stoichiometric variations around other already known quasicrystals and approximants. Furthermore, all known quasicrystals are synthetic; no natural quasicrystal has ever been found. A more systematic way to search for quasicrystals, including natural quasicrystals, is desirable, and one way is to search through collections of diffraction data. Although a two-dimensional electron diffraction pattern would immediately show a quasicrystal's salient forbidden symmetry, no large collection of such patterns exists. However, a collection of over eighty thousand *powder* diffraction patterns in digital form, the powder diffraction file (ICDD-PDF), is published by the International Center for Diffraction Data. The catalog contains synthetic inorganic and organic phases, as well as some nine thousand mineral patterns. Because the powder diffraction pattern of a material averages over all orientations, only the magnitude (and not the direction) of the scattering vector in reciprocal space is preserved, and a quasicrystal's distinctive noncrystallographic symmetry cannot be observed directly. *A priori,* it is unclear if quasicrystals can be identified from their powder diffraction patterns alone.

In this Letter, we present a method to identify, classify, and index icosahedral quasicrystals based solely on their powder diffraction patterns. We apply the method to the ICDD-PDF and find the best-fit quasicrystal candidates. Our automated procedure picks out the known quasicrystals in the ICDD-PDF and, for the cases in which indexing has been published, produces the same indices. Although the remainder of the catalog is supposed to consist of periodic crystals, it was assembled over many years, including decades prior to the 1984 discovery of quasicrystals. Consequently, it is conceivable that the catalog includes some quasicrystals that were never identified as such. Based on our studies, we report promising materials.

The diffraction pattern of an ideal three-dimensional quasicrystal consists of Bragg peaks located on a lattice given by $\vec{Q} = \sum_{i=1}^{6} n_i \vec{b}_i$, where the $\vec{b}_i$ are basis vectors pointing to the vertices along the six fivefold symmetry axes of a regular icosahedron in three dimensions, and the n_i are integers that index each vector. The quasicrystal formula is similar to that for a crystal except that the number of basis vectors is greater than the number of dimensions (three), a consequence of the noncrystallographic symmetry. We choose the $\vec{b}_i$ following the convention in [3]:

$$\vec{b}_1 = (1, \tau, 0), \quad \vec{b}_2 = (\tau, 0, 1), \quad \vec{b}_3 = (0, 1, \tau),$$
$$\vec{b}_4 = (-1, \tau, 0), \quad \vec{b}_5 = (\tau, 0, -1), \quad \vec{b}_6 = (0, -1, \tau). \tag{1}$$

τ is the golden ratio, $(1 + \sqrt{5})/2$. An equivalent way to index the position of the three-dimensional reciprocal-space scattering vector is to use a scheme analogous to crystallographic Miller $(h\ k\ l)$ indices. Six integer indices grouped into pairs describe the distance along Cartesian basis vectors, $\vec{Q} = (h + h'\tau)\hat{x} + (k + k'\tau)\hat{y} + (l + l'\tau)\hat{z}$. The $(h/h'\ k/k'\ l/l')$ indices are permutations of the n_i:

$$h = n_1 - n_4, \quad h' = n_2 + n_5, \quad k = n_3 - n_6,$$
$$k' = n_1 + n_4, \quad l = n_2 - n_5, \quad l' = n_3 + n_6. \tag{2}$$

Because the $(h/h'\ k/k'\ l/l')$ indices express distances along Cartesian axes, the advantages of orthogonal coordinate axes are conveniently recovered. Also, associated with every $\vec{Q}$ is a vector $\vec{Q}_\perp$, constructed from another integer linear combination of the same basis vectors: $\vec{Q}_\perp = (h' - h\tau)\hat{x} + (k' - k\tau)\hat{y} + (l' - l\tau)\hat{z} = \sum_{i=1}^{6} n_i \vec{b}_i^{\perp}$, where

$$\vec{b}_1^{\perp} = (-\tau, 1, 0), \quad \vec{b}_2^{\perp} = (1, 0, -\tau), \quad \vec{b}_3^{\perp} = (0, -\tau, 1),$$
$$\vec{b}_4^{\perp} = (\tau, 1, 0), \quad \vec{b}_5^{\perp} = (1, 0, \tau), \quad \vec{b}_6^{\perp} = (0, \tau, 1). \tag{3}$$

In powder diffraction patterns, the reciprocal space is collapsed to one dimension, where all vectors with the same magnitude $|\vec{Q}|$ are degenerate. The magnitude $|\vec{Q}| \equiv Q$ is the reciprocal of the d spacing, the quantity listed in the entries of the ICDD-PDF. Q^2 and $|\vec{Q}_\perp|^2 \equiv Q_\perp^2$ can now be expressed as integer linear combinations of only two basis vectors, whose lengths are related by the golden ratio: $Q^2 \propto N + \tau M$ and $Q_\perp^2 \propto N\tau - M$, where $N = 2\sum_{i=1}^{6} n_i^2$ and $M = h'^2 + k'^2 + l'^2 + 2(hh' + kk' + ll')$. Each peak in a quasicrystal powder diffraction pattern can be indexed by the two integers N and M. The entire diffraction pattern can be scaled by a factor of τ^3 along the Q direction, and the support will remain the same, a consequence of the self-similarity of the pattern. That is, for each lattice vector at position $Q^2 = (N, M)$, there is another lattice vector of similar intensity at position $(N', M') = \tau^6 Q^2$. Using the relation $\tau^2 = \tau + 1$,

$$\begin{aligned}(N', M') &\equiv N' + M'\tau = \tau^6(N + M\tau) \\ &= (5M + 8N) + (8M + 13N)\tau \\ &\equiv (5M + 8N, 8M + 13N)\,. \end{aligned} \tag{4}$$

Although three other different indexing schemes persist in the literature to describe icosahedral quasicrystal powder patterns [4–6], they are all analytically equivalent to the convention given here.

There are three distinct icosahedral reciprocal lattices: simple icosahedral (SI), face-centered icosahedral (FCI), and body-centered icosahedral (BCI). The SI, FCI, and BCI reciprocal lattices correspond to real-space lattices obtained by, for example, placing identical "atoms" at each lattice point of a simple hypercubic, a face-centered hypercubic, and a body-centered hypercubic lattice in six dimensions, respectively, and projecting down to three dimensions. (In [7], the SI, FCI, and BCI lattices are referred to as P*, I*, and F*, respectively.) For these primitive lattices, the intensity is given by [8]

$$I \propto \left[\frac{\sin(Q_\perp/2)}{Q_\perp/2}\right]^2. \tag{5}$$

Note that I increases as $Q_\perp \to 0$ so that bright peaks — the ones likely to be observed experimentally — have small $Q_\perp$. Equation (5) does not account for chemical and other effects that modulate the intensities in the diffraction pattern of a real material, but it provides a guide as to which peaks should be observed when testing real patterns.

Testing patterns.—The first step in testing a real powder pattern is to find the best possible peak-by-peak match between that pattern $\{Q_i\}$ and the perfect quasicrystal template pattern $\{q_i\}$. Then, various statistical tests can be applied to compare that match to what is expected for a true quasicrystal.

If we were to match to a periodic crystal template pattern, the test would be more straightforward. For any finite interval of Q over which a pattern is measured, a real crystal has a finite number of diffraction peaks. One also has good *a priori* estimates for the nonzero minimum distance between nearest peaks, which is set by the lattice constant. These features, useful in matching the template to the real pattern, allow a unique indexing.

For the quasicrystal, the process is more complicated because the number of peaks in any finite interval of the ideal pattern is infinite (the pattern is dense) and, consequently, there is no uniquely defined lattice constant or indexing. How does one sensibly match a real pattern, with a finite number of peaks in a given interval ΔQ, to a quasicrystal template pattern, with a dense set of peaks in that same interval? One must account for the intensity of the peaks, not just their Q. Although the quasicrystal powder pattern is dense, most of its peaks within any finite interval of Q have a large $Q_\perp$ and are predicted by Eq. (5) to be too dim to distinguish from the noise present in any real experiment. So, instead of finding the template $q_{i'}$, which comes closest to the observed Q_i (i.e., minimizing $|Q_i^2 - q_{i'}^2|$ alone), we instead minimize $|Q_i^2 - q_{i'}^2|/I_{i'}$, which includes the intensity $I_{i'}$ of the i'th template peak. This approach tends to match real Q_i to the nearest *bright* peaks in the template pattern, naturally accounting for phason shifts, imperfections, and experimental error that may shift Q_i from its ideal value and cause an incorrect assignment to some $q_{i'}$ with an unrealistically small intensity.

The procedure for finding the best match between the real and template patterns, then, is as follows. Choose some bright peak in the ideal pattern (N_0, M_0) with a low value of N. An "attempted match" consists of rescaling its magnitude to match the first real peak in the pattern, Q_1. Identify each remaining peak $Q_{i\neq 1}$ in the real pattern with the template peak $q_{i'}$ which minimizes $|Q_i^2 - q_{i'}^2|/I_{i'}$. Next, introduce a goodness-of-fitness parameter S_1 to characterize the attempted match between the $\{Q_i\}$ and the $\{q_{i'}\}$. Repeat the process by assigning (N_0, M_0) to the second real peak Q_2 and compute its goodness of fit, S_2. After repeating for each real peak, use the lowest S_j to decide the best overall match between the real pattern and template. Each real peak Q_i is now assigned the set of indices $\{n_{i'}\}$ or, equivalently, $\{N_{i'}, M_{i'}\}$ of the matching template peak.

The goodness-of-fit parameter S_j depends on $\bar{\Delta} = \langle |Q_i - q_{i'}|/Q_i \rangle$, where $\langle \mathcal{O}_i \rangle$ denotes an intensity-weighted average $(\sum_i \sqrt{I_i}\,\mathcal{O}_i)/(\sum_i \sqrt{I_i}\,)$. $\bar{\Delta}$ measures the fractional deviation between Q_i and $q_{i'}$ and is weighted by intensity for the same reasons as above. (Results do not change significantly if $\sqrt{I_i}$ is replaced by I_i or some similar function of intensity.) One challenge is that for each good fit of Q_i to a template peak $q_{i'}$ labeled by (N, M), there is also an equally good fit to the peak $\tau^{6k}(N, M)$ where k is any integer, due to the self-similarity of the lattice; see Eq. (4). This leads to the practical problem of deciding which match to choose and also the annoyance that, unlike a crystal, the indexing is not unique. To produce a unique and sensibly standardized indexing, we simultaneously

minimize $\bar{N} = \langle N_i \rangle$. The goodness of fit S can be taken to be a linear combination of these two parameters, $S = a\bar{\Delta} + \bar{N}$. The results are relatively insensitive to the choice of a (up to an order of magnitude) provided that the $\bar{\Delta}$ and $\bar{N}$ contributions to S are both non-negligible for known quasicrystals; typical values are $\bar{N} \approx 30$ and $\bar{\Delta} \approx 0.3$, and we used $a = 500$ throughout.

If the real material is a crystal, the best attempted match to the quasicrystal template (corresponding to the lowest S_j) is still a poor match relative to a true quasicrystal, so we next introduce statistical tests to measure the quality of the match. These tests were found empirically by applying them first to known quasicrystals, and they involve calculating several quantities for each pattern. The first two statistical quantities, $\bar{\Delta}$ and $\bar{Q}_\perp$ (the intensity-weighted average of $Q_\perp$), are discussed above. Quasicrystals have low values of both, representing closer matches to brighter peaks. However, finite resolution limits the number of peaks present above the noise level; while these two parameters clearly separate out FCI quasicrystals (see Fig. 1), they fail for the SI case, where 1700 patterns score better than known SI quasicrystals when ranking only by these two statistics. We therefore consider another quantity that involves interrelations among the bright peaks in a quasicrystal powder pattern.

Each peak in a powder pattern has a parity determined by $\eta \equiv \sum_i n_i$. Even (odd) η corresponds to even (odd) parity. Over a finite interval, certain sequences of even and odd peaks appear. For a given bright peak at Q_0, there are other bright peaks at $Q = Q_0 + \Delta Q$, where $\Delta Q \equiv \Delta N + \Delta M\tau \equiv (\Delta N, \Delta M)$. All of these peaks should have low values of $Q_\perp$ and will therefore be separated by small $\Delta Q_\perp^2 = \Delta N\tau - \Delta M$. $\Delta M/\Delta N$ should approximate τ, the golden ratio, and, as is well known, the best approximant is a ratio of subsequent Fibonacci numbers. Hence, for every peak in the powder pattern, we look for other peaks separated by "Fibonacci intervals" $(\Delta N, \Delta M)$, where ΔN and ΔM are either successive Fibonacci integers or constant multiples of these integers. In the SI case, we search for two types of intervals: those occurring between peaks of opposite parity, which involve successive Fibonacci numbers, such as $(2, 3)$ and $(34, 55)$, and those occurring between peaks of the same parity, which involve four times successive Fibonacci numbers, such as $(8, 12)$ and $(20, 32)$. In the FCI and BCI cases, only even-parity peaks are present, and we seek only sequences with four times successive Fibonacci integers.

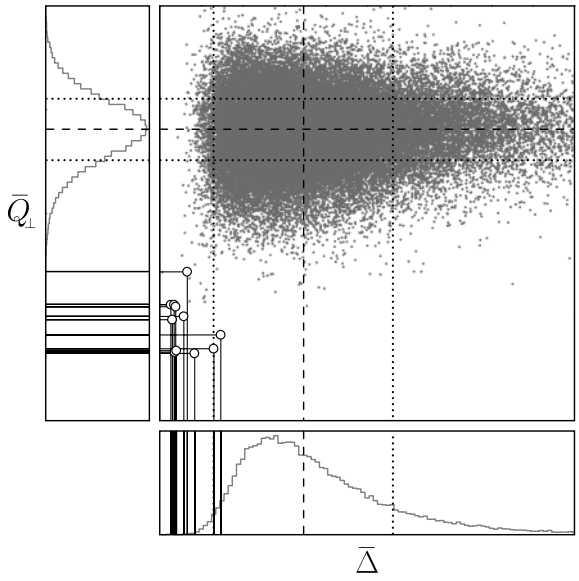

FIG. 1. A plot of the distribution of quantities $\bar{\Delta}$ and $\bar{Q}_\perp$ for eleven patterns identified as FCI quasicrystals in the ICDD-PDF (white circles) and 60 000 patterns identified as crystals (grey dots). The large square shows the scatter plot in the two-dimensional parameter space, in arbitrary units with the origin at lower left. Rectangles along either axis show the individual histograms of $\bar{\Delta}$ and $\bar{Q}_\perp$. Means and standard deviations for each individual quantity are marked by dashed and dotted lines, respectively. The quasicrystals are projected to show that they lie at the tail of the distributions.

For each ith peak in the real pattern, we count the number of other real peaks that are separated from it by one of the Fibonacci intervals. If there is only one such peak, then the ith peak is considered part of a pair (or 2-plet); if two, part of a 3-plet, etc. We define $M_i^{(m)}$ to be 1 if the ith peak is part of an m-plet and zero otherwise. Note that $M_i^{(m)} = 1$ implies $M_i^{(m-1)} = 1$. For example, if the ninth peak in a pattern is separated from three other peaks by Fibonacci intervals, then $M_9^{(2)} = M_9^{(3)} = M_9^{(4)} = 1$ and $M_9^{(5)} = 0$. The values of $M_i^{(m)}$ for each peak are combined into intensity-weighted averages $\bar{M}^{(m)} = \langle M_i^{(m)} \rangle$.

The three average quantities $\bar{\Delta}$, $\bar{Q}_\perp$, and $\bar{M}^{(4)}$ are unified into a single χ^2 statistic, which quantifies the degree of quasicrystallinity of a powder x-ray diffraction pattern. First, the distribution for each quantity, calculated for all 60 000 entries in the ICDD-PDF with a dozen peaks or more, is fit to a standard Gaussian by matching percentiles. Then, χ^2 is calculated from the three normalized measures. All patterns with any worse-than-average quantity are discarded and the remaining patterns with a high value of χ^2 represent patterns with characteristics most like those of the known quasicrystals.

Results.—The χ^2 statistic has proven to be a reliable method of identifying and indexing quasicrystal diffraction patterns. For example, Fig. 1 shows a scatter plot of $\bar{\Delta}$ vs $\bar{Q}_\perp$ for 60 000 patterns from the ICDD-PDF. The eleven patterns known to be synthetic quasicrystals of the FCI structure (by checking the references given in the ICDD-PDF) are represented by white circles; the remaining patterns are shown in grey. The clustering of the eleven quasicrystals apart from the remaining points demonstrates the success of the tests in separating out quasicrystal patterns. The few grey dots around the white quasicrystal circles are patterns identified as crystalline in the ICDD-PDF that might be misidentified quasicrystals.

TABLE I. Top quasicrystal candidates for SI, FCI, or BCI lattices. Type refers to whether candidates were labeled in the ICDD-PDF as quasicrystal, synthetic crystal, or mineral crystal. Shown are a typical quasicrystal, and the top five synthetic and top mineral candidates. The best known quasicrystals have χ^2 values up to 154.8 (SI) and 397.8 (FCI).

PDF num	Formula	Lattice	Type	χ^2
New data [9]	CdYb	SI	QC	34.7
27-901	$SnTe_3O_8$	SI	Syn	28.4
42-842	InP_3	SI	Syn	27.9
44-583	$CaUO_4$	SI	Syn	27.4
21-117	$Cd(MnO_4)_2 \cdot 6H_2O$	SI	Syn	21.4
38-923	K_2NaPdF_6	SI	Syn	19.8
25-298	Aktashite, $Cu_6Hg_3As_4S_{12}$	SI	Min	17.9
48-1437	$Al_{68.5}Pd_{22.1}Mn_{9.4}$	FCI	QC	92.0
40-106	$Ba_3La_{40}V_{12}O_{93}$	FCI	Syn	40.3
19-261	$CaYb_2O_4$	FCI	Syn	38.9
31-1420	UO_3	FCI	Syn	34.1
41-979	$Cr_{0.9}Ta_{5.1}S$	FCI	Syn	33.8
27-863	$Sr_7Y_{13}O_4(PO_4)_3(SiO_4)_9$	FCI	Syn	33.7
2-691	Tantalite, $(Fe, Mn)Ta_2O_6$	FCI	Min	25.2
21-379	InPtU	BCI	Syn	40.1
50-1135	$Co_4Sn_{13}Tb_3$	BCI	Syn	36.2
42-1163	$Pb_{10}Al_2F_{25}Cl$	BCI	Syn	26.8
45-1164	$Al_{20}Mo_{1.656}Th$	BCI	Syn	25.9
36-1231	$LaNiO_2$	BCI	Syn	24.9
44-1412	Gratonite, $Pb_9As_4S_{15}$	BCI	Min	14.3

However, many of these possibilities are eliminated when the remaining $\bar{M}^{(4)}$ test is applied. Because no one or two tests are completely effective, we combine three quantities into a χ^2 statistic.

Table I lists the top quasicrystal candidates for the SI, FCI, and BCI structures. For each structure, the list includes a typical example of a known quasicrystal (except BCI, where none is known), the top five synthetic materials identified as crystalline, and the top mineral candidate in the ICDD-PDF. The ranking should not be taken as an absolute measure. Different versions of the statistical tests can alter the ranks of some promising candidates, sometimes significantly, but those shown remain among the top ranked throughout. Our quasicrystal example in the SI case is the recently discovered binary alloy, CdYb [9]. Interestingly, a stoichiometrically similar phase, (ostensibly crystalline) Cd_6Yb, placed seventh in the BCI top candidate list. For the BCI case, there is no known quasicrystal, and though the top candidates have high values of χ^2, the χ^2 values cannot be compared directly between different structures since statistical tests are different. Nevertheless, the high scores suggest followup studies of the best candidates, particularly InPtU and $Co_4Sn_{13}Tb_3$.

A further success is that our automated indexing of peaks for the known quasicrystals matches the available published indices. In some cases, while the published indices are aided by two-dimensional diffraction data, our automated procedure uses powder data only. Given the unique challenges in quasicrystal indexing, described earlier, the successful indexing suggests that our matching of template and real patterns automatically incorporates standards obtained by individual analysis. Hence, as more quasicrystals are discovered and added to catalogs, our procedure could provide a standardized indexing.

Future work will proceed in several directions. A number of materials merit further study, and, intriguingly, the most promising examples are in the BCI class where no quasicrystal has yet been found. Systematic studies of synthetic materials with nearby stoichiometries may also be merited. Finally, we are collecting the powder diffraction patterns of other materials, including known quasicrystals and crystal approximant phases, to further refine our tests. We are interested in collaborating in exploring the leading candidates, only some of which have been given in Table I. Those interested are encouraged to contact P. J. L. and P. J. S.

We thank the ICDD for providing the ICDD-PDF; P. Tandy (Natural History Museum, London), J. Post (Smithsonian), and L. Cabri (CANMET) for lending us mineral samples for pilot studies; and A.-P. Tsai for sending us the CdYb powder pattern. P. J. L. thanks B. Fujito and M. Yogo for help with coding and statistics, respectively. This work was supported in part by the U.S. Department of Energy Grant No. DE-FG02-91ER40671 (P. J. S.) and NSF MRSEC Grant No. DMR-94-00362 (N. Y.).

*Current address: Department of Physics, Jefferson Laboratory, Harvard University, 17 Oxford Street, Cambridge, MA 02138.
Electronic address: plu@fas.harvard.edu

[1] D. Levine and P. J. Steinhardt, Phys. Rev. Lett. **53**, 2477 (1984).
[2] A. I. Goldman and P. A. Thiel, in *Quasicrystals: The State of the Art,* edited by D. P. DiVincenzo and P. J. Steinhardt (World Scientific, Singapore, 1999), pp. 561–601.
[3] C. Janot, *Quasicrystals: a Primer* (Oxford University Press, New York, 1994), 2nd ed.
[4] P. A. Bancel, P. A. Heiney, P. W. Stephens, A. I. Goldman, and P. M. Horn, Phys. Rev. Lett. **54**, 2422 (1985).
[5] J. W. Cahn, D. Shechtman, and D. Gratias, J. Mater. Res. **1**, 1 (1986).
[6] V. Elser, Phys. Rev. B **32**, 4892 (1985).
[7] N. D. Mermin, in *Quasicrystals: The State of the Art* (Ref. [2]), pp. 137–195.
[8] D. Levine and P. J. Steinhardt, Phys. Rev. B **34**, 596 (1986).
[9] A. P. Tsai, J. Q. Gyo, E. Abe, H. Takakura, and T. J. Sato, Nature (London) **408**, 537 (2000).